OBSERVING THE SUN AT 20–650 MHZ AT THERMOPYLAE WITH ARTEMIS

A. KONTOGEORGOS[1], P. TSITSIPIS[1], X. MOUSSAS[2,*], G. PREKA-PAPADEMA[2], A. HILLARIS[2], C. CAROUBALOS[3], C. ALISSANDRAKIS[4], J.-L. BOUGERET[5] and G. DUMAS[5]

[1]*Department of Electronics, Technological Educational Institute of Lamia, Lamia 35100, Greece*
[2]*Department of Physics, University of Athens, Athens 15783, Greece*
[3]*Department of Informatics, University of Athens, Athens 15783, Greece*
[4]*Department of Physics, University of Ioannina, Ioannina 45110, Greece*
[5]*LESIA, Observatoire de Paris, Observatoire de Paris-Meudon, Meudon Cedex 92195, France*
([*]Author for correspondence, E-mail: xmoussas@phys.uoa.gr)

(Received 26 September 2005; Accepted in final form 20 February 2006)

Abstract. Fine structure of type IV radio solar bursts with a great variety and complexity often give much information in different ways and enable estimation of various coronal characteristics. In this work, we expose our new method for fine structure revealing and separation of two basic kinds of type IV fine structure, as fibers and pulsations. We also estimate frequency drift of fibers from dynamic spectra, clean from continuous background, with a prototype method using 2-D Fourier transform and we estimate periodicities of fibers as well as pulsations with continuous wavelet transform. Working with the last method we found periodicities close to 3 min umbral oscillations and 5 min global solar oscillations.

Keywords: special issue WSEF sun, solar radio bursts, solar flares, radio spectrograph, fibers, pulsations, coronal loop oscillations

1. Introduction

It is well known that type IV radio solar bursts have a strong radio background with complicated parameters such as start time, duration and time evolution of spectral limits (McLean and Labrum, 1984). However, a more complex aspect related to this kind of solar radiation is fine structure, due to the fact that usually this is weak enough and is often buried in the much more intense background. Many kinds of fine structure have been reported at meter wavelengths as well as at higher frequencies (Jiřička *et al.*, 2001; Aurass *et al.*, 2003). Among all these fine structures *fibers* and *pulsations* possess a dominant position, due to their frequent appearance during great solar events, as well as due to their long duration and perhaps the correlation with other solar effects. *Fibers* reveal as threads with intermediate frequency drift in dynamic spectra. They are very interesting fine structures that are observed in strong type IV radio solar bursts usually after the maximum of radio flux. They are produced as the result of interaction of Langmuir waves with whistlers (Kuijpers, 1975; Bernold and Treuman, 1983), but many dark points exist in their behavior.

Space Science Reviews (2006) 122: 169–179
DOI: 10.1007/s11214-006-7492-8

Pulsations are characteristic evidences of coronal loop oscillations and have been studied for many years now with unimpaired interest (Roberts *et al.*, 1984; Wright and Nelson, 1987; Zaitsev *et al.*, 1998; Kliem *et al.*, 2000; Zlotnik *et al.*, 2003). They reveal as quasi-linear structures with an extremely high frequency drift in dynamic spectra, usually high intensity and almost uninterrupted presence during type IV solar bursts.

In the next section, we present the instrumentation of ARTEMIS (Section 2), whereas in the next three sections we describe three basic areas of investigation, namely, fine structure revealing and separation (Section 3), estimation of frequency drift and exciter velocity for fibers (Section 4), and study of periodicities of long-term quasi-periodic bursts (Section 5).

2. Instrumentation

The improved ARTEMIS solar radio spectrograph of the University of Athens operates in the area of Thermopylae Satellite Station of OTE (Greek Telecom Organizarion). It is a complete system that receives and records the dynamic spectrum of solar radio emission every day, covering a frequency bandwidth of 20–650 MHz and it consists of two antennas, two receivers, and two personal computers (PCs) equipped with analog-to-digital (A/D) converters (Figure 1).

2.1. Antennas

The solar radio spectrograph has a parabolic and a dipole antenna. The parabolic one has a diameter of 7 m and covers a range of received frequencies 100–650 MHz. It is fed by a log-periodic antenna, which consists of 13 dipoles in a total length of 2.25 m. The overall mean gain achieved is 21 dB, whereas the mean half power beam width is about 6°. Antenna has a typical equatorial mounting and follows the Sun. The signal after receiving is routed to band pass filters and multistage amplifiers. Every morning the system is self-calibrated and automatically starts the antenna movement. The dipole antenna is a stationary very fat inverted V dipole, on the east–west plane. Each leg has length 3.5 m, width 1 m and is made of copper tube. The two legs form a 90° corner and its apex is 3.6 m above ground. During all the day antenna receives the sun radio signals, as well as a lot of interfering signals because it is almost omnidirectional. After receiving, the signal is routed to a floating band pass filter ($f_H = 90$ MHz, $f_L = 20$ MHz). An active balun-broadband amplifier follows and a combiner combines the signals from the two antennas and drives them to the control room through a 70 m transmission line.

2.2. Receivers and Data Acquisition

The signal enters into the control room through the transmission line. There, it follows two different ways. First way includes a classical sweep frequency analyzer

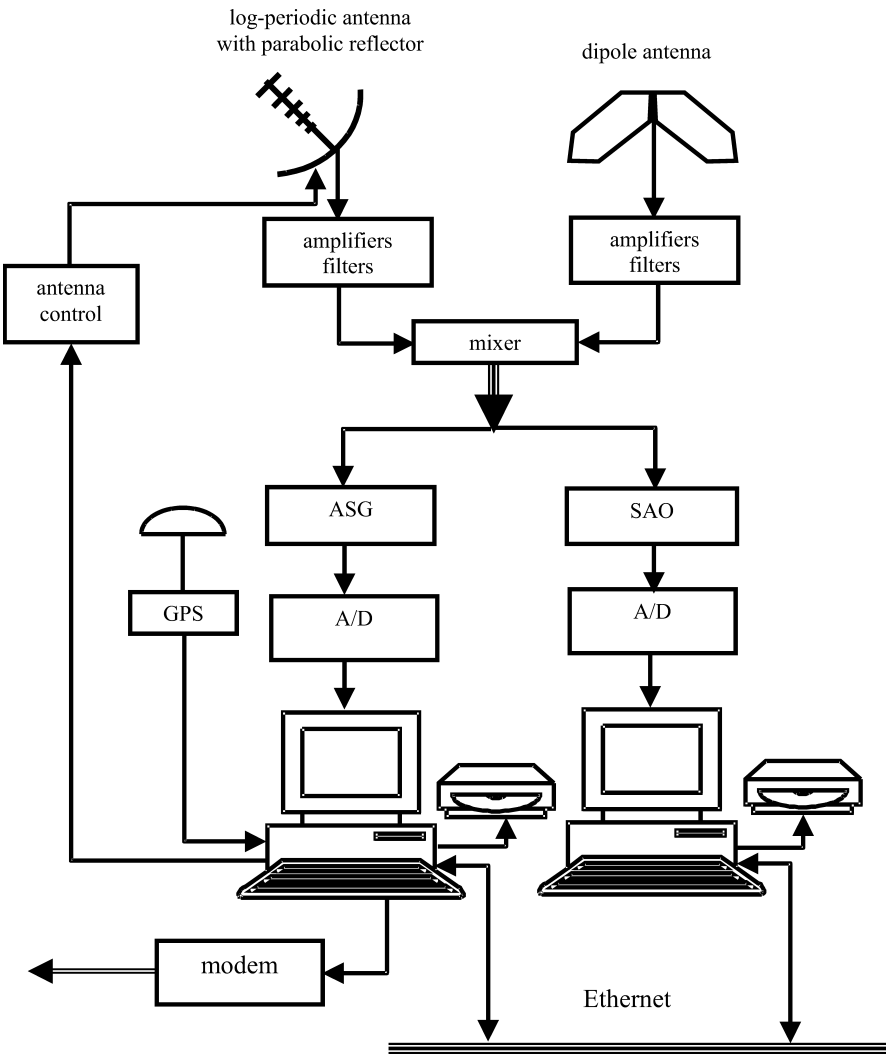

Figure 1. Presentation of ARTEMIS in a simplified block diagram.

(Analyseur de Spectre Global, ASG) which receives the whole range from 20 to 650 MHz at 10 sweeps/s with instantaneous bandwidth of 1 MHz and dynamic range of 70 dB. The analog output from the ASG drives a 12 bit, A/D card on a PC (Figure 1). It gets 6,300 samples/sweep. Samples are averaged in tenths, so as the whole spectrum (20–630 MHz) is divided into 630 channels with resolution bandwidth of 1 MHz. We also take care to avoid strong FM radio and TV interference. Total sensitivity is about $30 \times 10^{-22}\,\mathrm{Wm}^{-2}\,\mathrm{Hz}^{-1} = 30\,\mathrm{sfu}$. After five sweeps, data are transferred to the hard disk with universal time (UT) stamp. The daily data is about 0.5 GB. Every day, before start of measurements, this PC receives the UT

from a GPS, controls the calibration and the antenna movement. This PC is equipped with a telephone line modem for telemetry purposes and is connected to the latter through an ethernet local network connection. Second way includes a pass band filter, RF amplifier, and finally an acousto-optic frequency analyzer (Spectrograph Acousto-Optic, SAO) for 270–450 MHz frequency range, with low dynamic linear range (20 dB), very good frequency resolution (176 kHz), and very fast frame rate (100 Hz). Every 10 ms 1,024 samples are recorded with a resolution of 12 bits and they are averaged every eight samples, so as 128 channels be performed with resolution bandwidth of 1.4 MHz. This arrangement leads to a high signal-to-noise ratio. Every 50 sweeps the data are transferred to the hard disk with a UT stamp. The daily data are about 1 GB. The UT is received every morning from the other PC through the ethernet local network.

3. Fine Structure Revealing and Separation

Fine structure revealing and seperation includes processing of data recorded by ARTEMIS-IV solar radio spectrograph. This is a 2-D directional high pass filtering, applied to horizontal (time) direction, so as continuous radio background and slow time variations of radio flux be removed and fine structure be visible. Term "2-D (two dimensional) directional filtering" means a kind of two-dimensional filtering where the impulse response of the filter is not omnidirectional but exhibits an obvious anisotropy. A characteristic representative of this kind of filters is that one, which along a determined direction has the impulse response given by Equation (1) (x represents distance along radial direction), whereas it becomes zero for all other directions. A similar filter but for a "one-dimensional" signal corresponding to a specific radio frequency is also used by Abrami and Koren (1978). The filter used in our method is called "high pass gaussian filter" because of the equation describing it. Its advantage is fine frequency response, especially in the cut-off region, which is clear of side lobes. Impulse response of this filter is given by the relation

$$h_{\mathrm{HP}}(x) = -\frac{1}{\sigma\sqrt{2\pi}}\, e^{-\frac{x^2}{2\sigma^2}}, \qquad x = -m, \ldots -1, 1, \ldots m$$
$$h_{\mathrm{HP}}(0) = 1 - \frac{1}{\sigma\sqrt{2\pi}} \tag{1}$$

where σ is the standard deviation of gaussian distribution and $2m + 1$ is the filter length. Filter optimization gives $\sigma \cong m/6$, so as to avoid additional terms with almost zero values, which, however, could increase the processing time. So, the only parameter that could vary is the length of the filter determined by the variable m. Length of the filter $2m+1$ has to be bigger enough relatively to the signal details, but also smaller enough of the slowly varying components so as to reject them. In most cases of our applications $m = 50$ gives quite good results for removing continuous background as well as radio interference (Figure 2). This value corresponds to

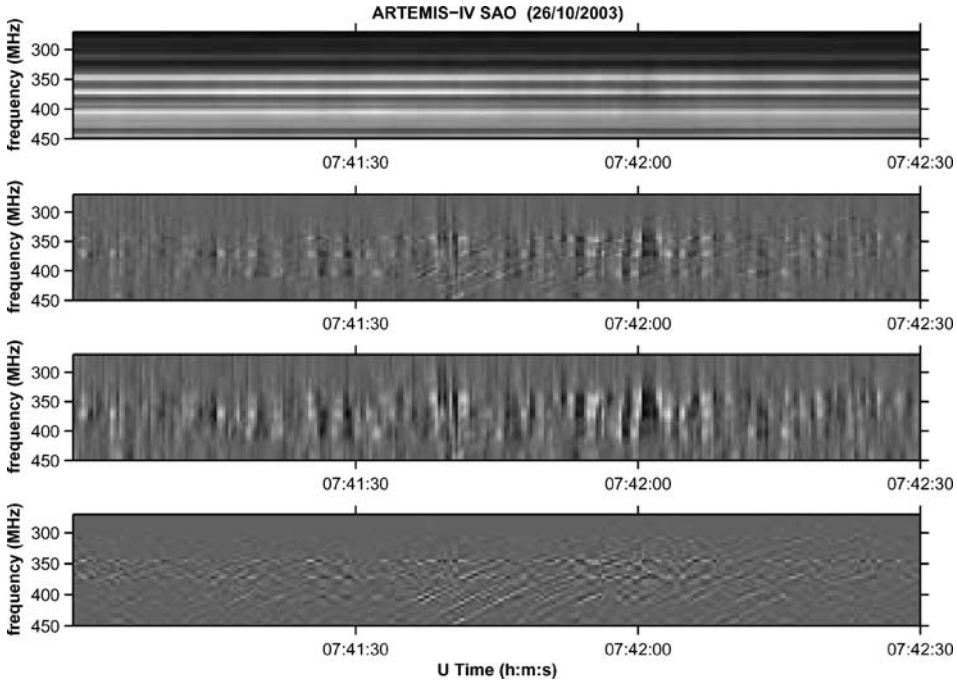

Figure 2. Revealing of fine structure of type IV radio solar burst. *Top panel*: Original dynamic spectrum recorded by ARTEMIS-IV SAO on October 26, 2003 (07:41:00–07:42:30 UT). Recognition of fine structure is impossible. *Second panel*: Fine structure hidden in the previous dynamic spectrum is revealing after directional filtering. *Third panel*: Pulsations existing in the previous dynamic spectrum is separated from the rest fine structure with directional filtering. *Bottom panel*: Fibers existing in the previous dynamic spectrum are revealing after subtracting image of the third panel from the image of the second panel.

a filter length of 101 points, which means time duration of about 5 s for a time sampling rate of 20 spectra/s and direction of filter is 0° (horizontal). Limitations resulting from the above description are related with direction and length of the filter. This filter rejects all linear structures, which have the same direction with it, whereas reveal all other linear structures. It has best results for linear structures perpendicular to the filter direction, but results are fairly acceptable for direction close to filter direction. Filter cannot reject very short linear structures with the same direction (linear structures with length too shorter than the length of the filter). Also, revealing of structures is quite difficult for very wide linear structures (width of structure not smaller than the filter length).

The same method, namely 2-D directional filtering, is used for separation of the two main kinds of fine structure. Separation is very important because, very often, these two fine structures appear at the same time in dynamic spectra and each structure and its time behavior can be studied individually. Results of fine structure revealing and separation of fibers and pulsations are shown in Figure 2.

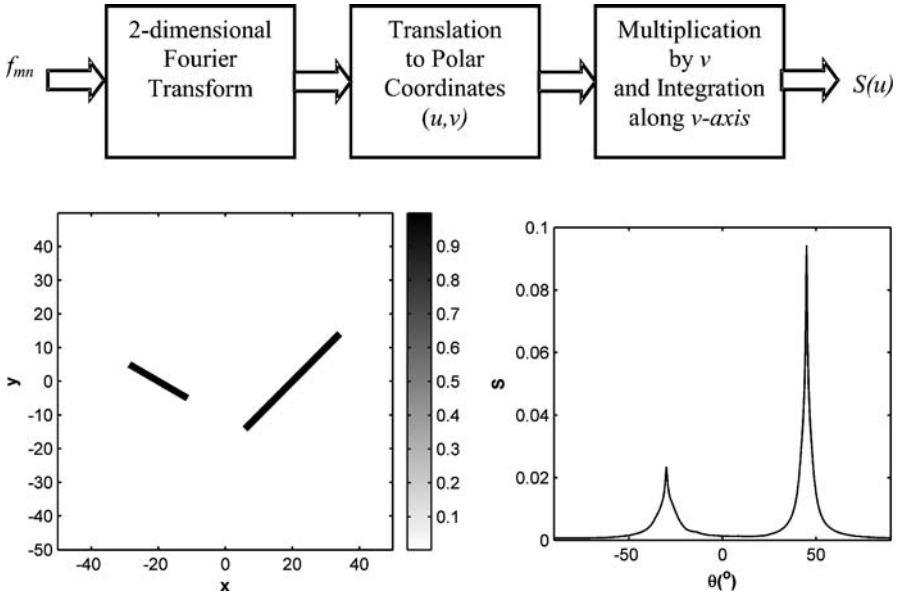

Figure 3. Top panel: Basic steps in estimation of "angular spectrum" of an original image representing fine structure. *Bottom panel*: Application of algorithm to a prototype image representing two line segments at angles -30° and 45°, respectively (*left*) produces an "angular spectrum" forming two peaks at -30° and 45°, respectively. Height of peaks is proportional of the total "energy" in corresponding angle value.

4. Estimation of Frequency Drift and Exciter Velocity for Fibers

The method used is based on the fact that traces of fibers in dynamic spectra have a linear or quasi-linear shape that is performed by movement of exciters upwards or sometimes downwards in solar corona and specifically in magnetic loops. We used a prototype method based on 2-D Fourier transform that is applied to dynamic spectra having linear or quasi-linear structures. Specifically, for every segment of dynamic spectrum that includes interesting bursts, we derive the 2-D Fourier transform. Next, this 2-D signal is transformed to polar coordinates and is integrated across radial direction (Figure 3, top panel). The result is a function representing the "energy" of the original image for all angles and is given by the relation

$$S(\theta) = 2 \int_0^\infty |F(\xi, \theta)|^2 \, \xi \, d\xi \tag{2}$$

where (ξ, θ) are polar coordinates in Fourier space and $F(\xi, \theta)$ is the 2-D Fourier transform of the original image translated to polar coordinates (Tsitsipis *et al.*, 2005). As we see, magnitude $S(\theta)$ is a function of angle θ, one of the polar coordinates and this is the reason we call it "angular spectrum." Different angles could be translated to corresponding slopes so as the corresponding "slope spectrum" of

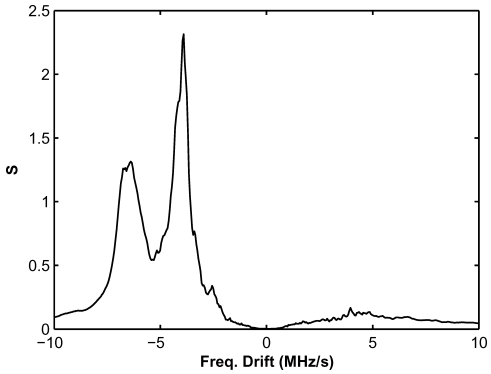

Figure 4. "Slope spectrum," referred to dynamic spectrum of Figure 2 (*bottom panel*), derived with our method based on 2-D Fourier transform. Two major groups of fibers are well defined forming frequency drifts of −3.9 and −6.4 MHz/s for mean emission frequencies 315 and 405 MHz, and give exciter velocities of 5.1×10^6 and 5.8×10^6 m/s, respectively.

the original image is derived. This means that linear structures of a specific slope give a peak at the angular/slope spectrum at the corresponding value of angle/slope (Figure 3, bottom panel). Height of peaks is proportional of the "energy" of linear structures that have the particular slope. Slope spectrum of the dynamic spectrum of Figure 2 (bottom panel) is shown in Figure 4 and is referred to as a piece of dynamic spectrum (ARTEMIS-IV SAO, October 26, 2003) with duration of 1.5 min (07:41:00–07:42:30 UT). The whole process is fully automatic, which means that a sequence of these spectra can be produced for a specific event, giving so a "time evolution" of slopes of fibers.

Using a coronal density model (Newkirk, 1961) and the fact that plasma emission is the emission mechanism for this metric radiation, it is proved that frequency drift is a function of the exciter velocity. This method is used by Tlamicha and Karlický (1976) in order to estimate the exciter velocity of type II solar burst, but could also apply to fiber bursts because they are produced by plasma emission too. Tlamicha and Karlický supposed emission of fundamental radiation, but we modify it for use for the second harmonic, because radio radiation in second harmonic is the more probable hypothesis for the frequency region 270–450 MHz of our dynamic spectra. Fundamental plasma emission could not exist at frequencies so high as 450 MHz. So, frequency drift defined by quasi-linear pattern of fibers are given by relation (3)

$$\frac{df}{dt} = -\frac{f}{19.9s}\left[\ln\left(0.148\frac{f^2}{s^2}\right)\right]^2 V \tag{3}$$

where df/dt is the frequency drift, f the frequency of the emission of radiation at any time, s the number of harmonic (=2), and V is the exciter velocity. We use this relation to estimate the exciter velocity corresponding to each frequency drift. Frequency range is the operation region of ARTEMIS-IV SAO, which permits high time resolution, very important for drift detection. So, each "slope spectrum"

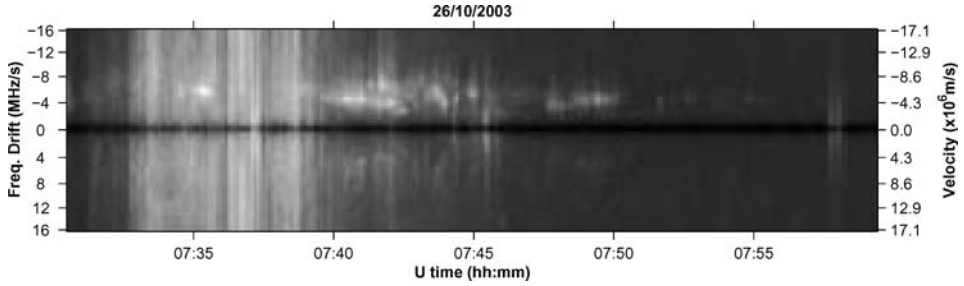

Figure 5. Evolution of frequency drifts as well as exciter velocity of fibers vs. time for a time period of 30 min (07:30–08:00 UT) during type IV radio solar burst of October 26, 2003.

(Figure 4) is translated to a "velocity spectrum" referred to the exciter velocity of fiber bursts. Next, we construct the evolution of drifts during a time period where we focus, which can be translated to the evolution of exciter velocity with the help of Equation (3), modified so as emission in second harmonic is assumed. We can see a sample of this evolution image in Figure 5.

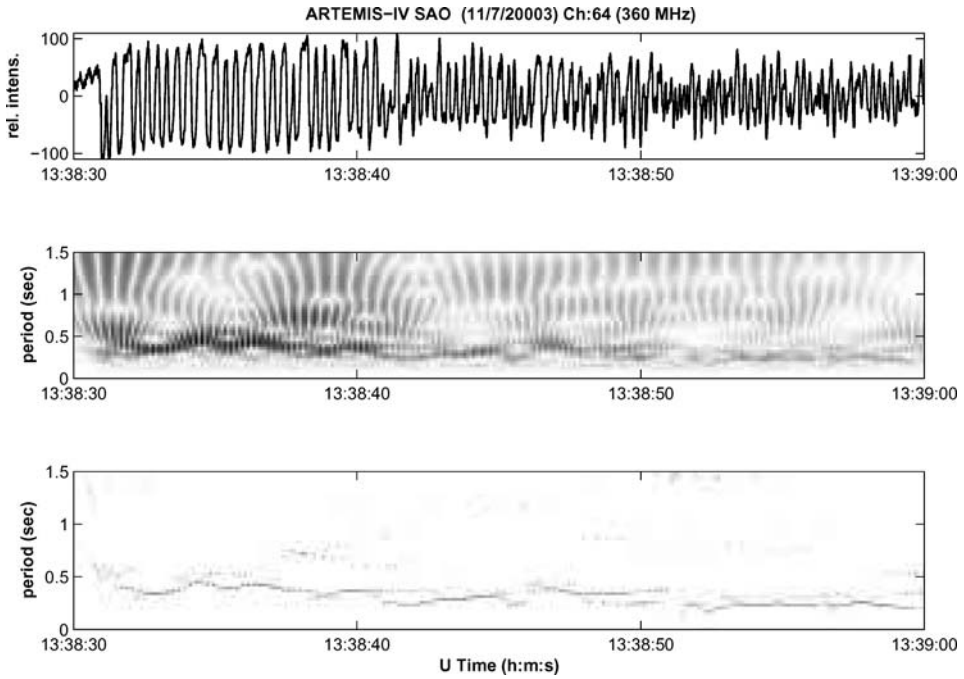

Figure 6. Periodicity of pulsations for a 30-s duration during type IV solar burst of July 11, 2000 recorded by ARTEMIS IV SAO. It refers to channel 64 (360 MHz). (a) Original signal after removing of continuous background. (b) Spectral analysis with continuous wavelet transform. (c) Skeleton of previous figure graph where a small but evident decrease of period is shown.

5. Study of Periodicities of Long-Term Quasi-Periodic Bursts

Pulsations as well as fibers demonstrate a quasi-periodical repetition (Roberts *et al.*, 1984; Wang and Xie, 1997; Kuijpers, 1975). Most of them have a period of about 0.5 s that is varying from a fraction of 1 s to a few seconds. These periods are due to oscillations in fast sausage mode, usually in higher harmonics taking place at the coronal loops apexes (Wang, 2004). There are no significant variations of this period during a particular event, but minor variations for shorter time periods are observed (Figure 6).

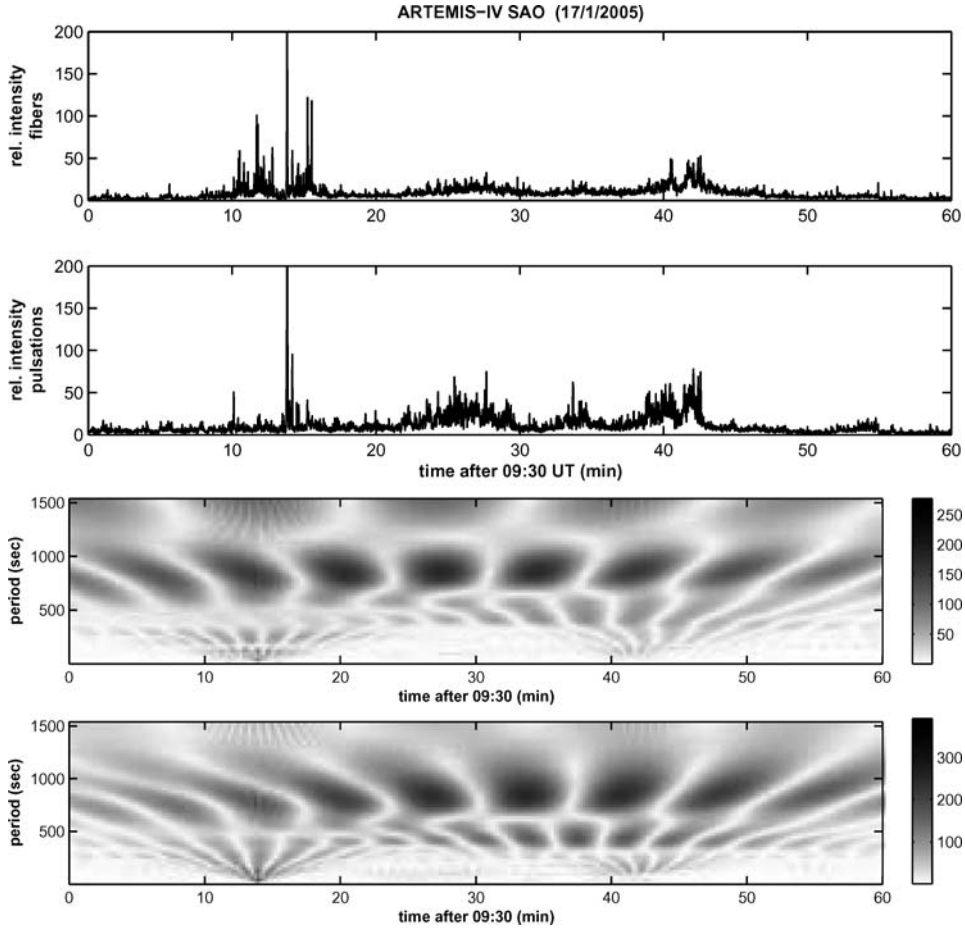

Figure 7. Long-term periodicities of fibers and pulsations during type IV solar burst of January 17, 2005. Relative intensity (rms) of (a) fibers and (b) pulsations. Spectral analysis of (c) fibers and (d) pulsations.

In order to study periodicities of exciter that are inducted to pulsations as well as to fiber bursts, we use root mean square (rms) of signal for a particular channel with integration over a time period of 1 s (Figure 7, top two panels). So, we found periodicities of some minutes that depend on the particular event, using continuous wavelet transform (Kaiser, 1994; Mallat, 1998) as the method of analysis (Figure 7, two bottom panels).

From this spectral analysis, periods of 99, 260, 400, and 850 s are detected for fibers and 118, 246, 395, and 828 s are detected for pulsations. These periodicities are consistent with observations of DeMoortel *et al.* (2002a) and Nakariakov (2004) who are working on 171 Å TRACE recordings and are produced probably by longitudinal or slow kink oscillations of coronal loops, which are driven by sunspot oscillations and global solar oscillations (DeMoortel *et al.*, 2002a,b; Nakariakov, 2004).

6. Conclusions

Type IV radio solar bursts have a great variety of fine structure that might help in estimation of physical parameters of solar corona. Directional filtering could help in revealing fine structure, as well as in isolating various coexisting fine structures. Estimation of frequency drifts of fibers during type IV radio solar bursts is a fast method and leads to estimation of exciter velocities of fibers. These velocities vary from about 1×10^6 to 30×10^6 m/s and have usually negative values, which means that exciters move outwards in solar corona. Positive values are fewer and weaker. Fibers reveal usually after radio flux maximum and this is consistent with the assertion that they are formed on postflare loops. Wavelet transform is a convenient tool for study of periodicities of quasi-periodic bursts, as fibers and pulsations are. Periodicities of about 250 and 400 s are found, which are consistent with 3 min of umbra oscillation and 5 min of global solar oscillations.

Acknowledgements

We express our thanks to the University of Athens Grant Committee for financial support.

References

Abrami, A. and Koren, U.: 1978, *Astron. Astrophys. Suppl.* **34**, 165–179.
Aurass, A., Klein, K.-L., Zlotnik, E. Ya., and Zaitsev, V. V.: 2003, *Astron. Astrophys.* **410**, 1001–1010.
Bernold, T. and Treumann, R.: 1983, *Astrophys. J.* **264**, 677–688.
DeMoortel, I., Hood, A. W., Ireland, J., and Walsh, R. W.: 2002a, *Solar Phys.* **387**, L13–L16.

DeMoortel, I., Ireland, J., Hood, A. W., and Walsh, R. W.: 2002b, *Astron. Astrophys.* **209**, 89–108.
Jiřička, K., Karlický, M., Mészárasová, H., and Snížek, V.: 2001, *Astron. Astrophys.* **375**, 243–250.
Kaiser, G.: 1994, *A Friendly Guide to Wavelets*, Birkhauser, Boston.
Kliem, B., Karlický, M., and Benz, A. O.: 2000, *Astron. Astrophys.* **360**, 715–728.
Kuijpers, J.: 1975, *Solar Phys.* **44**, 173–193.
Mallat, S.: 1998, *A Wavelet Tour of Signal Processing*, Academic Press, New York.
Mc Lean, D. J. and Labrum, N. R.: 1984, *Solar Radiophysics*, Cambridge Press, Cambridge.
Nakariakov, V. M.: 2004, Theoretical Aspects of MHD Coronal Seismology, In *Proceedings of SOHO 13 - Waves, Oscillations and Small-Scale Transient Events in the Solar Atmosphere: A Joint View from SOHO and TRACE*, Palma de Mallorca, Ballearic Islands, Spain, ESA SP-547, ESA Publications Division ESTEC, Noordwijk, pp. 407–416.
Newkirk, G.: 1961, *Astrophys. J.* **133**, 983–1013.
Roberts, B., Edwin, P., and Benz, A.: 1984, *Astrophys. J.* **279**, 857–865.
Tlamicha, A. and Karlický, M.: 1976, *BAICz* **27**, 6–10.
Tsitsipis, P., Kontogeorgos, A., Hillaris A., Moussas, X., Caroubalos, C., and Preka–Papadema, P.: 2005, *Pattern Recognit.* (revised).
Wang, M. and Xie, R. X.: 1997, *Solar Phys.* **176**, 171–179.
Wang, T.: 2004, Coronal Loop Oscillations: Overview of Recent Results in Observations, In *Proceedings of SOHO 13 – Waves, Oscillations and Small-Scale Transient Events in the Solar Atmosphere: A Joint View from SOHO and TRACE*, Palma de Mallorca, Ballearic Islands, Spain, ESA SP-547, ESA Publications Division ESTEC, Noordwijk, pp. 417–426.
Wright, C. and Nelson, G.: 1987, *Solar Phys.* **111**, 385–395.
Zaitsev, V. V., Stepanov, A. V., Urpo, S., and Pohjolainen, S.: 1998, *Astron. Astrophys.* **337**, 887–896.
Zlotnik, E., Zaitsev, V., Aurass, H., Mann, G. and Hofmann, A.: 2003, *Astron. Astrophys.* **401**, 1011–1022.